

Aerodynamic Admittance Function of Tall Buildings

Yin Zhou^a Ahsan Kareem^b

^a *Malouf Engineering Int'l, Inc., 175 W. Campbell Rd, Richardson, TX, USA*

^b *NatHaz Modeling Laboratory, University of Notre Dame, Notre Dame, USA*

ABSTRACT: The aerodynamic admittance function (AAF) has been widely invoked to relate wind pressures on building surfaces to the oncoming wind velocity. In current practice, strip and quasi-steady theories are generally employed in formulating wind effects in the along-wind direction. These theories permit the representation of the wind pressures on building surfaces in terms of the oncoming wind velocity field. Synthesis of the wind velocity field leads to a generalized wind load that employs the AAF. This paper reviews the development of the current AAF in use. It is followed by a new definition of the AAF, which is based on the base bending moment. It is shown that the new AAF is numerically equivalent to the currently used AAF for buildings with linear mode shape and it can be derived experimentally via high frequency base balance. New AAFs for square and rectangular building models were obtained and compared with theoretically derived expressions. Some discrepancies between experimentally and theoretically derived AAFs in the high frequency range were noted.

KEYWORDS: Aerodynamic admittance function; Wind effects; Tall Buildings; Turbulence; Wind tunnel; Code and Standard

1. INTRODUCTION

The aerodynamic admittance function (AAF) has been widely invoked to relate wind pressures on building surfaces to the oncoming wind velocity in the frequency domain [6]. In current wind engineering practice, strip and quasi-steady theories are generally employed in formulating analysis of wind effects in the along-wind direction following the “gust loading factor” (GLF) approach [1,2,7]. The application of these assumptions permitted the representation of the wind pressure field on the building surface completely by the oncoming wind velocity field. Figure 1a illustrates the chain relationship among various loading and response features [2,8]. The effectiveness of these assumptions has been examined by limited field measured data [3, 5] as well as wind tunnel model pressure tests [4,7]. Synthesis of the wind velocity field utilizing its covariance and auto-spectral descriptions leads to a generalized wind load (GWL) that employs the AAF or GWL-AAF in the GLF formulation. This paper first reviews the theoretical background of the development of current GWL-AAF to identify some inherent variations and discrepancies. This is followed by a comparison of GWL-AAFs used in several major international codes and standards, which exhibit a considerable scatter. Since the GWL-AAF has an inherent shortcoming in its definition, therefore, no experimental validation of this function is available as it depends both on the mode shape and frequency (Figure 1a). In this paper, a new definition of AAF is presented, which is based on the base bending moment (BBM). It is noted in Figure 1b that the BBM-AAF is independent of the mode shape in contrast with the GWL-AAF. The BBM-AAF is numerically equivalent to the current GWL-AAF for most code applications due to implied assumption of linear mode shape [10]. Furthermore, the BBM-AAF can be derived using wind tunnel tests employing a high frequency base balance.

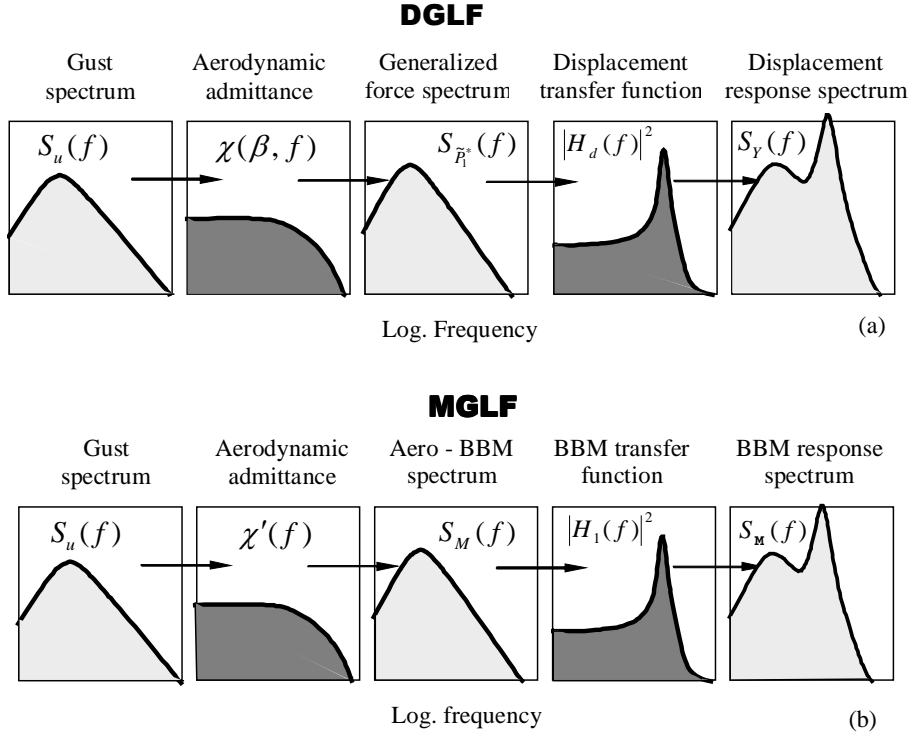


Figure 1. Aerodynamic admittance functions in gust loading (a) DGLF; (b) MGLF.

2. THEORETICALLY-DERIVED AAF

2.1. Wind pressures on buildings

Using strip and quasi-steady theories, the structure of wind pressures on building surface is replaced with that of the oncoming wind (Figure 2). In particular, the wind load per unit height at any height z is treated as proportional to the square of the velocity at that height

$$\hat{P}(z, t) = 1/2 \rho \hat{V}^2(z, t) \cdot C_d \cdot B \quad (1)$$

where $\hat{P}(z, t) = \bar{P}(z) + \tilde{P}(z, t)$ = peak externally applied wind load in which \bar{P} = mean wind load and \tilde{P} = zero-mean fluctuating component of wind load; t = time; $\hat{V}(z, t) = \bar{V}(z) + v(z, t)$ = peak wind velocity in which \bar{V} = mean wind velocity and v = zero-mean fluctuating wind velocity; ρ = air density; C_d = drag force coefficient; and B = width of building normal to the oncoming wind. The mean wind velocity is usually expressed in the form of $\bar{V}(z) = \bar{V}_H (z/H)^\alpha$ where \bar{V}_H = mean wind velocity evaluated at the building height H and α = exponent of mean wind velocity profile.

When neglecting the contribution of the quadratic fluctuating wind velocity term, the fluctuating wind load can be written as

$$\tilde{P}(z, t) = \rho \bar{V}(z) \cdot v(z, t) \cdot C_d \cdot B \quad (2)$$

which is a combined wind force including wind pressures in both windward and leeward faces or

$\tilde{P}(z, t) = \int_0^B (p_w(x, z, t) + p_l(x, z, t)) dx$ as shown in Figure 2, in which p = wind pressure; and

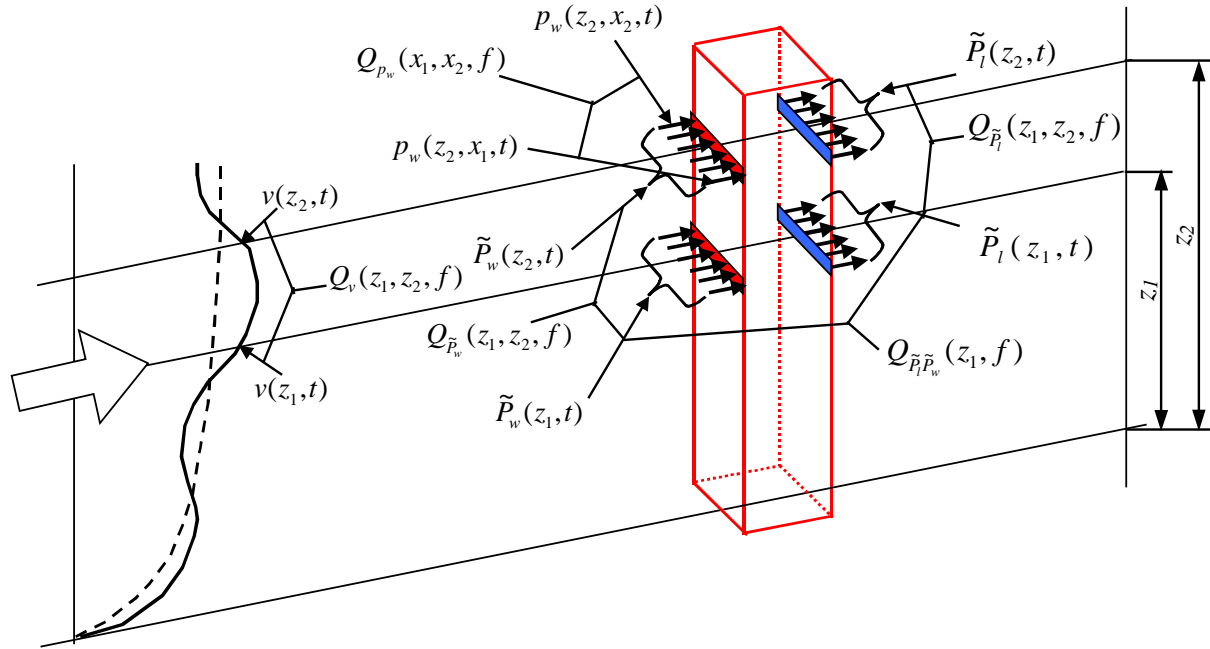


Figure 2. Structure of wind velocity and pressure on a tall building

subscripts w and l indicate windward and leeward, respectively. In the frequency domain, the following spectral relationship can be introduced

$$S_{\tilde{p}}^*(z, f) = C_{\tilde{p}} \cdot S_v^*(z, f) \cdot \chi_{\tilde{p}}(z, f) \quad (3)$$

where $S_{\tilde{p}}^*(z, f)$ = normalized spectrum of fluctuating wind load per unit height at height z ; $S_v^*(z, f)$ = normalized spectrum of wind velocity; $\chi_{\tilde{p}}(z, f)$ = AAF with regard to unit wind load; and $C_{\tilde{p}}$ = a coefficient. The correlation structure of unit wind loads at different heights can be expressed by

$$S_{\tilde{p}}(z_1, z_2, f) = S_{\tilde{p}}(z_1, f) \cdot S_{\tilde{p}}(z_2, f) \cdot Q_{\tilde{p}}(z_1, z_2, f) \quad (4)$$

where $S_{\tilde{p}}(z_1, z_2, f)$ = cross-spectral density of wind loads per unit height between height z_1 and z_2 ; and $Q_{\tilde{p}}(z_1, z_2, f)$ = correlation of wind load which is replaced by that of the wind velocity or $Q_{\tilde{p}}(z_1, z_2, f) = Q_v(z_1, z_2, f)$ according to the strip and quasi-steady theories.

2.2. Generalized Wind Loading Based AAF

Utilizing the above wind pressure information, a GWL is usually computed in deriving the “gust loading factor” (GLF) for along-wind load effects

$$S_{\tilde{p}'}(f) = \int_0^H \int_0^H S_{\tilde{p}}(z_1, z_2, f) \cdot \varphi_1(z_1) \varphi_1(z_2) dz_1 dz_2 \quad (5)$$

where \tilde{p}' = GWL in the fundamental mode; and the fundamental structural mode shape of a building assumed to be in the form $\varphi_1(z) = c(z/H)^\beta$ in which β = mode shape exponent and c = normalization factor. In most of current codes and standards, a linear mode shape is assumed or $\beta = 1$. A GWL-AAF can be evaluated as

$$\chi_{\tilde{p}'}(f) = C_{\tilde{p}'} \cdot S_{\tilde{p}'}^*(f) / S_v^*(f) \quad (6)$$

where $\chi_{\bar{p}'}(f)$ = GWL-AAF hereafter; $S_{\bar{p}'}^*(f)$ = normalized spectrum of the GWL; and $C_{\bar{p}'}$ = a coefficient. The above derivation shows that the GWL-AAF depends mainly on the correlation structure of wind pressures and the structural mode shape.

2.3. GWL-AAF in conventional GLF

Adopting the aforementioned GWL, the conventional GLF or DGLF, which is the ratio between peak wind-induced displacement and the mean, can be obtained. This form of the GLF has been widely used in almost all of the current wind loading codes and standards around the world following its presentation by Davenport [1,2]. For quick reference and comparison, a typical derivation of the DGLF is given in the Appendix. Expressions of the DGLF similar to that in (26) have been provided in most international codes and standards.

Based on the definition of DGLF in (17), the peak displacement response under the gusty wind is equal to the mean displacement multiplied by the DGLF. Similarly, referring to (20), the peak GWL can also be computed by

$$\hat{\mathbf{P}}' = G_Y \cdot \bar{\mathbf{P}}' = (1 + gr\sqrt{\mathbf{B} + \mathbf{R}}) \cdot \bar{\mathbf{P}}' \quad (7)$$

where $\hat{\mathbf{P}}'$ = peak GWL; G_Y = DGLF; $\bar{\mathbf{P}}'$ = mean GWL; g = peak factor; $r = 2I_{\bar{z}}$; $I_{\bar{z}}$ = turbulence intensity at a reference height of $\bar{z} \approx 2/3H$; \mathbf{B} = background factor; and \mathbf{R} = resonant factor which are all provided in the Appendix. For the background component the structural transfer function can be treated as to be unity. The RMS value of the background component is given by

$$\sigma_{\bar{\mathbf{P}}'_B} = r\sqrt{\mathbf{B}} \cdot \bar{\mathbf{P}}' = \sigma_{\bar{\mathbf{P}}'} \quad (8)$$

where $\sigma_{\bar{\mathbf{P}}'_B}$ = RMS background GWL component; and $\sigma_{\bar{\mathbf{P}}'}$ = RMS aerodynamic or externally applied GWL. Substituting (8) into (22) results in

$$\mathbf{K}_Y(\beta, f) = \mathbf{B} \cdot S_{\bar{\mathbf{P}}'}^*(f) / S_v^*(f) \quad (9)$$

Comparing (9) to (6), the GWL-AAF can be computed by

$$\chi_{\bar{\mathbf{P}}'}(f) = \mathbf{K}_Y(\beta, f) = |J_X(f)|^2 \cdot |J_Z(\alpha, \beta, f)|^2 \quad (10)$$

in which $|J_X(f)|^2$ and $|J_Z(\alpha, \beta, f)|^2$ = joint acceptance functions in horizontal and vertical directions, respectively, as expressed in (24) and (25).

A summary of GWL-AAFs in major international codes and standards is provided in Table 1 [9]. Since all GWL-AAFs in current codes and standards are developed based on a similar procedure as outlined in the Appendix, it is not surprising to notice that all GWL-AAFs are expressed in terms of very similar functions involving the size of buildings in the horizontal and vertical directions. However, since different codes and standards have employed significantly different wind parameters, these details have led to apparent scatter in the GWL-AAFs.

3. BASE BENDING MOMENT BASED AAF

Unlike the conventional DGLF which defines an equivalent static wind loading following exactly the distribution of the mean wind force, a new MGLF has been introduced by the authors [8]. Among other advantages, this new MGLF can provide more realistic equivalent wind loading for dynamically-sensitive structures. The new MGLF is defined as the ratio between the

Table 1. GWL-AAFs in major international codes and standards

	Expressions of GWL-AAF
ASCE 7	$\chi(f) = R_H R_B (0.53 + 0.47 R_D)$ $R_l = 1/\eta - 1/2\eta^2(1 - e^{-2\eta}), \eta > 0; R_l = 1, \eta = 0$ $R_H, \eta = 4.6fH/V_{\bar{z}}; R_B, \eta = 4.6fB/V_{\bar{z}}; R_D, \eta = 15.4fD/V_{\bar{z}}$
AS1170.2	$\chi(f) = \frac{1}{\left(1 + 3.5fH/\bar{V}_H\right) \cdot \left(1 + 4fB/\bar{V}_H\right)}$
NRCC	$\chi(f) = \frac{1}{\left(1 + 8fH/(3\bar{V}_H)\right) \cdot \left(1 + 10fB/\bar{V}_H\right)}$
RLB-AIJ	$\chi(f) = \frac{0.84}{\left(1 + 2.1fH/\bar{V}_H\right) \cdot \left(1 + 2.1fB/\bar{V}_H\right)}$
Eurocode	$\chi(f) = R_H R_B$ <p style="text-align: center;">R_H and R_B are the same as those in ASCE7.</p>

peak base bending moment response and the mean. Using procedure similar to the derivation of the DGLF, a MGLF can be derived and expressed in similar form as in (26). Applying the MGLF to the BBM response, the background BBM component can be expressed as

$$\sigma_{MB} = \sqrt{\mathbf{B} \cdot r \cdot \bar{M}} = \sigma_M \quad (12)$$

where σ_{MB} = RMS background BBM response; \bar{M} = mean BBM; and σ_M = RMS aerodynamic BBM. Meanwhile, the following relationships relevant to the BBM-AAF can be obtained:

$$\chi_M(f) = \mathbf{K}_M(f) = |J_X(f)|^2 \cdot |J_Z(\alpha, 1, f)|^2 \quad (13)$$

$$\chi_M(f) = \mathbf{B} \cdot \frac{S_M(f)/\sigma_M^2}{S_v(\bar{z}, f)/\sigma_v^2} \quad (14)$$

$$\mathbf{B} = \frac{\sigma_M^2}{(2I_{\bar{z}})^2 \cdot \bar{M}^2} \quad (15)$$

where $\chi_M(f)$ = BBM-AAF; and $S_M(f)$ = PSD of aerodynamic BBM. Two important features related to the BBM-AAF are noteworthy. Comparing (13) to (10), the BBM-AAF is exactly the same as the GWL-AAF for a building with linear mode shape, an assumption often implied in most current codes and standards. However, unlike the GWL-AAF that depends on some imaginary quantities such as the GWL, the BBM-AAF is only related to realistic quantities through (14) and (15). Meanwhile, the BBM-AAF depends on the overall wind pressure effects in terms of the BBM, without the need to know the detailed wind pressure structure. The equivalence between the GWL-AAF and the BBM-AAF provides the basis for experimental investigation of the GWL-AAF.

4. EXPERIMENTAL RESULTS

According to (14) and (15), the information needed for the derivation of BBM-AAF includes the input wind spectrum and turbulence intensity, as well as the BBM including both the mean and the fluctuating components. The later components can be perfectly measured with a strain type high frequency base balance (HFBB).

A 5-component HFBB was employed in wind tunnel tests involving two building models. Model 1 is a square model with $B = D = 100$ mm and Model 2 with $B = 100$ mm and $D = 150$ mm where D refers to the depth of the building model. Both models have a height of 600 mm. Two oncoming boundary layers were simulated corresponding to an open country terrain (BL1) and a city center (BL2), respectively. The input wind velocity and the base bending moments were measured simultaneously.

Figure 3 shows the test results for Model 1 in BL2 wind boundary. It is noted that the wind velocity spectrum follows the $f^{-5/3}$ rule closely in the high frequency region. Using the measured wind velocity and BBM spectra, the BBM-AAF is plotted against the theoretical GWL-AAF using the form provided by the NBC code or Davenport [2]. Notable differences between the tested BBM-AAF and the code based GWL-AAF can be noted in the high frequency region of interest to building analysts.

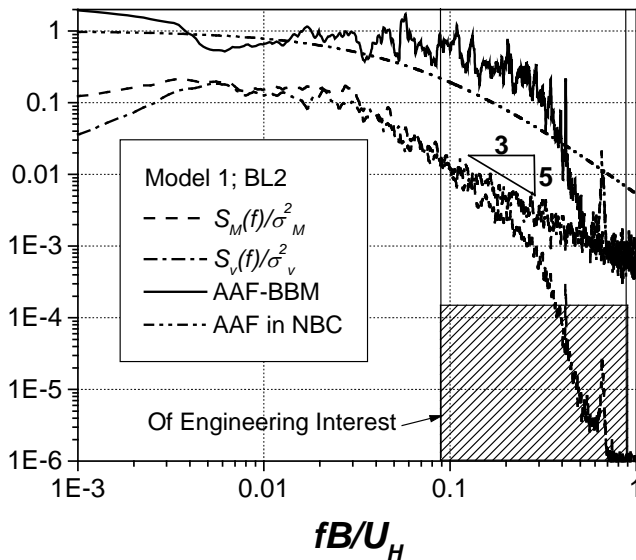


Figure 3. Wind spectrum, BBM spectrum and AAFs for a square building model

5. CONCLUDING REMARKS

The theoretical background in the development of GWL-AAF, which is used in current GLF based codes and standards, is first reviewed to identify relevant variations and discrepancies. Several major international codes and standards are compared in terms of their representation of GWL-AAFs, which exhibited considerable scatter. Since the GWL-AAF has intrinsic shortcomings in its definition and no experimental confirmation is available, this paper presented

a new concept of AAF that is based on the base bending moment (BBM). It was shown that the BBM-AAF was numerically equivalent to the current GWL-AAF for buildings with linear mode shapes, an assumption implied in most codes and standards. In addition, the BBM-AAF can be derived using measured BBM information. High frequency base balance wind tunnel tests were performed for a square and a rectangular building model. The BBM-AAF results obtained from this wind tunnel test were compared to the corresponding GWL-AAFs from codes and standards. Noteworthy discrepancies in the high frequency region between the measured and the theoretical AAF were noted. This suggested that the scatter in the response prediction of different codes and standards may be attributed in part to the choice of aerodynamic admittance function which did exhibit departure from those based on the strip and quasi-steady theories.

6. APPENDIX: AN TYPICAL DERIVATION OF DGLF

In the current GLF approach, the ESWL on tall buildings is defined as the mean wind load multiplied by a magnification factor [2]

$$\hat{\mathbf{P}}(z) = G_Y \cdot \bar{\mathbf{P}}(z) \quad (16)$$

where $\hat{\mathbf{P}}$ = ESWL; G_Y = DGLF which can be computed by

$$G_Y = \hat{Y}(z) / \bar{Y}(z) = 1 + g \cdot \sigma_Y / \bar{Y} \quad (17)$$

where \hat{Y} and \bar{Y} = peak and mean displacement, respectively; g = peak factor which is usually about 3~4; and $\sigma_Y = \int_0^\infty S_Y(f) df$ = RMS displacement in which $S_Y(f)$ = PSD of displacement response. The DGLF takes into account the overall wind-structure-interaction including both structural dynamics and gust fluctuation.

Usually, the mean structural displacement can be approximated by that in the first mode

$$\bar{Y}(z) = (\bar{P}'_1 / k'_1) \cdot \varphi_1(z) \quad (18)$$

where $\bar{P}'_1 = \int_0^H \bar{P}(z) \varphi_1(z) dz$, $k'_1 = (2\pi f_1)^2 m'_1$ and $m'_1 = \int_0^H m(z) \varphi_1^2(z) dz$ are the GWL, stiffness and mass of the first mode, respectively; f_1 = natural frequency of the first mode; and $m(z)$ = mass per unit height.

Using the fluctuating GWL in (5) and following the framework in Fig. 2(a), the PSD of the fluctuating displacement in the first mode can be computed by

$$S_Y(z, f) = S_{\hat{P}}(f) \cdot |H_1(f)|^2 / k_1'^2 \cdot \varphi_1^2(z) \quad (19)$$

where $|H_1(f)|^2 = \left([1 - (f/f_1)^2]^2 + (2\zeta f/f_1)^2 \right)^{-1}$ = first mode structural transfer function; and ζ = critical damping ratio in the first mode. Combining (5) and (18) results in

$$\frac{S_Y(f)}{\bar{Y}^2} = \frac{S_{\hat{P}}(f)}{\bar{P}'_1{}^2} \cdot |H_1(f)|^2 \quad (20)$$

The integration of (20) is the fluctuating portion of the DGLF.

When assuming a full-correlation between the wind pressures on windward and leeward surfaces and using the detailed wind pressure description in (1)-(4), the PSD of the generalized wind load in (5) can be written as

$$S_{\tilde{p}}(f) = \int_0^H \int_0^H \int_0^B \int_0^B c^2 \rho^2 C_d^2 \bar{V}_H^2 \sigma_v^2 \left(\frac{z_1}{H}\right)^{\alpha+\beta} \left(\frac{z_2}{H}\right)^{\alpha+\beta} Q_X(x_1, x_2, f) Q_Z(z_1, z_2, f) S_v^*(z_1, z_2, f) dx_1 dx_2 dz_1 dz_2 \quad (21)$$

where $Q_X(x_1, x_2, f) = \exp\left(-\frac{C_X f}{\bar{V}(\bar{z})} |x_1 - x_2|\right)$ and $Q_Z(z_1, z_2, f) = \exp\left(-\frac{C_Z f}{\bar{V}(\bar{z})} |z_1 - z_2|\right)$ = horizontal and vertical correlation functions, respectively, in which C_X and C_Z = exponential decay coefficients; and \bar{z} = reference height. Substituting (21) and the mean GWL into (20) leads to

$$\frac{S_{\tilde{p}}(f)}{\bar{P}^{1/2}} = r^2 \cdot \mathbf{K}_Y(\beta, f) \cdot S_v^*(f) \quad (22)$$

where $r = 2I_{\bar{z}}$ in which $I_{\bar{z}} = \left((1 + \beta + 2\alpha)/(1 + \beta + \alpha)\right) \cdot I_H$, $I_H = \sigma_v / \bar{V}_H$ = turbulent intensity evaluated at height H ; and $\bar{z} \approx 2/3H$; and

$$\mathbf{K}_Y(\beta, f) = |J_X(f)|^2 \cdot |J_Z(\alpha, \beta, f)|^2 \quad (23)$$

in which $|J_X(f)|^2$ and $|J_Z(\alpha, \beta, f)|^2$ = joint acceptance functions in horizontal and vertical directions, respectively, that can be computed by

$$|J_X(f)|^2 = \frac{1}{B^2} \int_0^B \int_0^B Q_X(x_1, x_2, f) dx_1 dx_2 \quad (24)$$

$$|J_Z(\alpha, \beta, f)|^2 = \frac{(1 + \alpha + \beta)^2}{H^2} \int_0^H \int_0^H \left(\frac{z_1}{H}\right)^{\alpha+\beta} \left(\frac{z_2}{H}\right)^{\alpha+\beta} Q_Z(z_1, z_2, f) dz_1 dz_2 \quad (25)$$

It has been reported that the “(joint acceptance) functions fulfill the role of the aerodynamic admittance, but in addition, take into account the influence of mode shape on the effective excitation force” [2]. Substituting (20) and (22) into (17), and dividing the integration into background and resonant portions, the DGLF in codes and standards has been expressed by

$$G_Y = 1 + g \cdot r \cdot \sqrt{\mathbf{B} + \mathbf{R}} \quad (26)$$

where $\mathbf{B} = \int_0^\infty \mathbf{K}_Y(\beta, f) \cdot S_v^*(\bar{z}, f) df$ = background factor; and $\mathbf{R} = \pi S E / 4\zeta$ = resonant factor in which $E = f_1 S_v^*(\bar{z}, f_1)$ = gust energy factor and $S = \mathbf{K}_Y(\beta, f_1)$ = size reduction factor.

7. REFERENCES:

1. A. G. Davenport, The application of statistical concepts to the wind loading of structures, Proc. Inst. Civ. Engrs., 19 (1961)449-472.
2. A. G. Davenport, Gust loading factors, J. Struct. Div., ASCE, 93(3) (1967)11-34.
3. J. D. Holmes, Pressure fluctuations on a large building and along-wind structural loading. J. Indust. Aerodyn., 1(3) (1976).
4. A. Kareem, Synthesis of fluctuating along-wind loads on tall buildings, J. Engrg. Mech., ASCE, 112(1) (1986) 121-125.
5. H. Kawai, Pressure fluctuations on square prisms – applicability of strip and quasi-steady theories, J. Wind Engrg. Indust. Aerodyn., 13(1983).
6. H. W. Liepmann, On the application of statistical concepts to the buffeting problem, J. Aeronautical Sciences, 19(12) (1952) 793-800.
7. B. J. Vickery, Load fluctuations in turbulent flow, J. Engrg. Mech. Div., ASCE, 94(1) (1968) 31-46.
8. Y. Zhou, and A. Kareem, Gust loading factor: new model, J. Struct. Engrg., ASCE, 127(2) (2001) 168-175.
9. Y. Zhou, T. Kijewski, and A. Kareem, Along-wind load effects on tall buildings: A comparative study of major international codes and standards, J. Struct. Engrg., ASCE, 128(6) (2002a) 788-796.
10. Y. Zhou, A. Kareem, and M Gu, Mode shape corrections for wind effects on tall buildings, J. of Engineering Mechanics, ASCE, 128(1) (2002b).